Inner Ear Development in Cetaceans

Tara Thean[1], Nikolay Kardjilov[2], and Robert J. Asher[3]

[1](Corresponding author) Department of Zoology, University of Cambridge, Cambridge, UK

[2]Helmholtz-Zentrum Berlin, Berlin, Germany

[3](Corresponding author) Department of Zoology, University of Cambridge, Cambridge, UK

INNER EAR DEVELOPMENT, T. THEAN ET AL.

1 Summary

Cetaceans face the challenge of maintaining equilibrium underwater and obtaining sensory input within a dense, low-visibility medium. The cetacean ear represents a key innovation that marked their evolution from terrestrial artiodactyls to among the most fully aquatic mammals in existence. Using micro-CT data and histological data, we document shape and size changes in the cetacean inner ear during ontogeny, and demonstrate that, as a proportion of gestation time, the cetacean inner ear is precocial in its growth compared to that of suid artiodactyls. Cetacean inner ears begin ossifying and reach near-adult dimensions and shape as early as at 32 percent of the gestation period. Our earliest embryos with measurable inner ears (13 percent newborn length) exhibit a flattened cochlea (i.e. smaller distance from cochlear apex to round window) compared to later and adult stages. Inner ears of *Sus scrofa* have neither begun ossifying nor reached near-adult dimensions at 55 percent of the gestation period, but have an adult-like ratio of cochlear diameters to each other, suggesting an adult-like shape. The precocial development of the cetacean inner ear complements previous work demonstrating precocial development of other cetacean anatomical features such as the locomotor muscles to facilitate swimming at the moment of birth.

2 Keywords

3 Introduction

A central theme in cetacean research is the question of how cetaceans evolved to function entirely and exclusively in water. The fact of cetaceans' obligate aquatic nature is in part a function of what makes them instantly recognizable: their specialized anatomy (see Rose 2006 for review). Though biologists have made considerable progress in investigating cetacean anatomical modifications, many cetacean specialities remain incompletely understood.

One such speciality is the cetacean inner ear. Numerous studies have documented cetacean inner ear modifications (see, for example, Gray, 1907; Ketten & Wartzok, 1990; Ketten, 1992; Geisler & Luo, 1996; Lindenlaub & Oelschläger, 2000; Solntseva, 2002, 2010). Solntseva (1990) examines peripheral auditory system development in cetaceans and pinnipeds. Yamato & Pyenson (2015) and Kinkel et al. (2001) provide insight into cetacean middle ear ontogeny, and Solntseva (1999) documents how auditory structures form in terrestrial, semi-aquatic, and aquatic species. However, there are still gaps in the current understanding of cetacean inner ear ontogeny and evolution. As Cock (1966) notes, a full understanding of the genetic differences responsible for the variety of shapes and sizes present in adult animals requires ontogenetic history. Cetacean inner ears are particularly interesting because sound is a crucial means through which cetaceans receive input from their surroundings (Ketten, 1994) and because cetaceans need to move in a three-dimensional environment. Further, the cetacean ear region is able to perform sophisticated functions such as echolocation, particularly in odontocetes, and is extremely derived. Derivations of the cetacean inner ear alone are numerous. Among several derived features of the cetacean inner ear, Fleischer (1976) describes the low number of turns of cetacean cochleae, the extremely small cetacean semicircular canals (see also Spoor et al. 2002), and the unique odontocete and mysticete modes of cochlear coiling.

This paper examines cetacean inner ear ontogeny as it pertains to developmental events and growth allometry. We ask when during growth the cetacean inner ear takes on its adult shape and size, and how individual inner ear components scale with body size during ontogeny. Differences in developmental event timing and relative scaling during growth have contributed to work in mammalian evolution (see Hautier et al. 2012), life histories (see Lu, 2003), and functional morphology (see Melin et al. 2005), among other areas. Examinations of ontogenetic allometry in cetaceans are limited. Even studies that have addressed cetacean allometry from an ontogenetic standpoint have often done so only in postnatal specimens (see Clark & Odell, 1999; McLellan et al. 2002) — relatively few have examined foetal specimens as well (see Dunkin et al. 2005; Tsai & Fordyce, 2014; Yamato & Pyenson, 2015). There is relatively little information on how cetacean cranial morphology changes during foetal growth, though the studies on the topic

that exist (for example, Klima, 1995; Rauschmann et al. 2006; Armfield et al. 2011; Roston et al. 2013) have provided key insights into cetacean evolution and development.

Cetaceans are now strongly supported as aquatic artiodactyls — a group of even-toed terrestrial mammals that includes suiforms, tylopods, and ruminants — with hippopotamids as their closest living relatives (see Gatesy et al. 1999; Gingerich et al. 2001; Thewissen et al. 2001; Spaulding et al. 2009 for discussion). Lovell & Harper (2007) endorsed the use of *Sus scrofa* as a model against which to compare cetacean auditory systems, and Kandel & Hullar (2010) used *Bos taurus* to better understand the cetacean vestibular apparatus. As such, we examine inner ear ontogeny in *S. scrofa* as a comparison between terrestrial and obligate aquatic artiodactyls. We seek to observe changes in shape, size, and ossification onset in both whales and a closely related terrestrial artiodactyl (*S. scrofa*). Specifically, we examine whether the timing of ossification onset as well as developmental stage at which the organisms' ears attain adult proportion is conserved or labile between these species. This may shed light on mammalian developmental novelties and the role of the auditory and vestibular apparatus in aquatic life.

4   Methods

4.1   Three-dimensional data

We analyzed 29 unique, unsexed cetacean specimens, including adult petrosals (one specimen each of *Delphinapterus leucas* and *Phocoena phocoena*), a subadult skull (one specimen of *Megaptera novaeangliae*), and embryos or foetuses of up to 40cm in total length (10 specimens of *D. leucas*, four specimens of *Delphinus delphis*, one specimen of *Delphinus* sp., two specimens of *P. phocoena*, one specimen of *Hyperoodon ampullatus*, six specimens of *M. novaeangliae*, one specimen of *Balaenoptera borealis*, and one specimen of *Balaenoptera musculus*, as summarized in Table 1). Our samples for three-dimensional analysis included 20 odontocetes and nine mysticetes. We measured total length as the circumferential (rather than straight) distance between the tip of the rostrum to the tail fluke notch, similar to Yamato & Pyenson (2015), and followed Yamato & Pyenson (2015) in dividing

each specimen's total length by previously reported newborn total length measurements (see Table 1). We also analyzed four unique, unsexed *S. scrofa* specimens, including an adult skull, a postnatal skull, and two whole foetuses of 23 - 24cm crown rump length (CRL), measured from the top of the head to the tail base. Table 1 provides details of embryonic and foetal specimens.

We obtained three-dimensional data for all specimens using micro computed tomography (μCT) at the Helmholtz-Zentrum Berlin for Materials and Energy (HZB), the American Museum of Natural History (AMNH), and the Departments of Zoology and Engineering, University of Cambridge. We performed the scans with different spatial resolutions varying between 9.8 and 91μm depending on the sample size, collecting between 775 and 2316 reconstructed slices for each specimen. To obtain optimal contrast for the bone tissue we used X-ray energies of up to 100kV. We visualized the μCT data and created three-dimensional reconstructions of inner ear endocasts using the MIMICS Innovation Suite (Materialise's Interactive Medical Image Control System) medical imaging software. Due to software limitations we reduced the size of the TIFF format image stacks, first using the ImageJ "Binner" plugin (x and y shrink factors of 2, median pixel binning method), and then converting the slices from 16-bit to 8-bit images before importing them into MIMICS. This process resulted in a size reduction from ~19-25GB to ~1-4GB per stack. In creating three-dimensional reconstructions we used digital segmentation for those scans with fully and densely ossified petrosals as thresholding values were consistently different between tissue boundaries. We used manual segmentation for those scans in which the bony labyrinth was incompletely ossified, and thus whose tissue boundaries were gradients that were sometimes challenging to differentiate, to avoid the errors that would likely arise from insufficiently pronounced digital thresholding of boundaries.

Following Spoor et al. (2002), we chose the parameters cochlear slant height, first, second, and third (if appplicable) cochlear turn diameters, overall cochlea size, and semicircular canal radius of curvature to quantify inner ear anatomy (Figure 1). We also visually inspected each image stack to determine whether or not a specimen's bony labyrinth had ossified. To count the number of cochlear turns in each sample, we approximated the landmarks that Geisler & Luo (1996) used for this purpose. We defined the first landmark as the edge of the round

window closest to the "end" of the cochlea in three-dimensional reconstructions, approximating the beginning of the laminar gap that serves as the first landmark in Figure 5 of Geisler & Luo (1996). We took the second landmark to be the cochlear apex, following Geisler & Luo (1996). For those specimens whose bony labyrinths were very incompletely ossified, and thus produced thresholding gradients with noisy three-dimensional reconstructions in MIMICS, we estimated the number of cochlear turns from two-dimensional image stacks in the axial and coronal planes.

Cochlear slant height (Spoor et al. 2002) refers to the straight distance between the cochlear apex and the topmost edge (furthest from the apex) of the round window (Gray, 1907; Spoor et al. 2002; see Figure 1a). First, second, and third cochlear turn diameters refer to the largest diameter between the lumen centers of the first, second, and third cochlear turns respectively (see Figure 1b). To ensure consistent and comparable diameters across all specimens, we identified the best fit plane through the anterior semicircular canal (ASC) arc and translated this plane to the parts of the cochlea with the largest cochlear turn diameters, following Spoor (2014, pers. comm.; see Figure 1c). Specimens with cartilaginous bony labyrinths did not possess a clearly visible ASC in μCT. For these specimens, we estimated analogous planes to the ASC arc-best fit plane based on the position of the round window (when visible), the first and second cochlear turns, and the cochlear apex, following the suggestion of Spoor (2014, pers. comm.). Overall cochlea size refers to the mean of the slant height and the first, second, and third (if applicable) cochlear turn diameters (Spoor et al. 2002). Semicircular canal radius of curvature refers to the average of semicircular canal arc height and width, divided by two (Spoor et al. 2002; Spoor & Thewissen, 2008; Silcox et al. 2009), with arc height and width following the definitions of Spoor & Zonneveld (1995), slightly modified. We measured arc width perpendicular to arc height for all canals (see Figure 1d), and did not account for the angle of the measurements relative to the orientation of the lateral semicircular canal. Some specimens did not have sufficiently ossified bony labyrinths for accurate semicircular canal measurement.

We obtained three-dimensional data for 33 adult cetacean specimens and 1 adult *S. scrofa* specimen from Spoor et al. (2002). The cetacean specimens included *Eubalaena glacialis* (2), *Caperea marginalis* (1), *Eschrichtius robustus* (1), *Balaenoptera acutorostralis* (1), *Balaenoptera borealis* (1), *B. musculus* (1), *Bal-*

158 *aenoptera physalis* (1), *M. novaeangliae* (2), *Physeter catodon* (1), *Kogia* sp. (1),
159 *Berardius bairdii* (1), *Mesoplodon densirostris* (1), *Ziphius cavirostris* (1), *Pla-*
160 *tanista gangetica* (1), *Inia geoffrensis* (1), *Pontoporia blainvillei* (1), *D. leucas*
161 (1), *Monodon monoceros* (1), *Delphinus* sp. (2), *Feresa attenuata* (1), *Globi-*
162 *cephala* sp. (1), *Grampus griseus* (1), *Lagenorhynchus obliquidens* (1), *Orcinus*
163 *orca* (1), *Stenella* sp. (1), *Tursiops truncatus* (3), *Neophocaena phocaenoides* (1),
164 and *P. phocoena* (1).

4.2 Histological data

166 We analyzed four unique histological series of cetacean embryos from the Univer-
167 sity of Tübingen (one specimen of *Delphinus* sp., 1200 slices in total, 342 slices
168 covering one ear, slice distance 20μm, Azan-Heidenhain stain), University Museum
169 of Zoology, Cambridge, or UMZC (one specimen of *Balaenoptera* sp., 1683 slices
170 in total, 375 slices covering one ear, slice distance 15μm, haematoxylin and eosin
171 stain), and the Zoologisches Museum Berlin, or ZMB (two specimens of *M. no-*
172 *vaeangliae*, 990 slices in total, 158 slices covering one ear, slice distance unknown,
173 haematoxylin and eosin stain and 630 slices in total, 220 slices covering one ear,
174 slice distance unknown, haematoxylin and eosin stain). We analyzed one histologi-
175 cal series of a *S. scrofa* embryo (868 slices in total, 320 slices covering one ear, slice
176 distance 40μm, Azan-Heidenhain stain) from Tübingen. We photographed histo-
177 logical slides from Tübingen using a Canon EOS 600D camera, from the UMZC
178 using a Leica DFC420 camera, and from the ZMB using a Leica DFC490 camera,
179 and made measurements on those photographs using ImageJ.

180 Three-dimensional reconstructions with μCT data are possible due to sev-
181 eral factors, including the consistent inter-slice distance recovered between two-
182 dimensional reconstructions. Due to the inevitable uncertainties of working with
183 tissues that have been decalcified, dehydrated, stained, processed on a microtome,
184 mounted on glass slides, etc., it is not possible with most histological series to be
185 certain that every slice in a given stack is accounted for. Thus, 100 slices in a
186 series cut with a thickness of 20μa will almost certainly depart at least slightly
187 from 2mm of anatomy in the original specimen. For these reasons, we create
188 three-dimensional anatomical reconstructions from μCT data but not from our

histological specimens.

Due to the different slicing planes of the histological series, we could not translate the ASC arc plane to the part of the cochlea with the largest diameter of the turns. We therefore measured the cochlear diameters of the histological specimens in the planes in which they were originally sliced. For the *S. scrofa* specimen, which was sliced in an axial plane, we estimated the ASC arc plane from the histological slices in which the ASC arc was visible and translated that plane of measurement to the widest parts of the cochlear diameters. We did not measure slant height in the histological specimens because of the specimens' coronal slicing planes and/or the lack of a clearly visible round window in the slices, nor did we measure semicircular canal radii in the histological specimens, as the fact that we could not reslice the histological series according to a best fit plane through each canal meant that there was no way to ensure that we were taking measurements using the correct landmarks on the vestibule and individual canals.

We compared foetal inner ear measurements taken from three-dimensional and histological data to those of adults of the same species. We compared our inner ear measurements for *D. delphis* foetal specimens to those of adult *Delphinus* sp. We compared our inner ear measurements for the *Balaenoptera* sp. specimen to the mean inner ear measurements of adult *B. borealis* and *B. musculus*.

4.3 Staging, aging, and body mass

The embryonic and foetal specimens in this study were collected decades ago and thus lack data on individual age. Body length measurements, coupled with morphological observations such as external shape, enabled staging and aging of *D. delphis* embryos and foetuses according to the Stěrba et al. (2000) classification scheme. We estimated the ages of the *S. scrofa* foetuses using the Ullrey et al. (1965) prediction equation. To enable relative comparisons of foetal cetacean and *S. scrofa* growth with newborn individuals and to estimate how far along the gestation period foetuses were, we used mean gestation period and newborn and adult body length data for various cetacean species and *S. scrofa* from Struthers (1889), Ullrey et al. (1965), Ohsumi (1966), Jefferson et al. (1993), and Stěrba et al. (2000).

To enable visual comparison of bony labyrinth shapes between foetal and adult cetaceans as well as foetal and adult *S. scrofa* (Figures 4 and 5), we estimated the body masses of foetal specimens using the equation $W = aL^b$ proposed by Schultz (1938) to predict the weights of large fish and whales, where W is body weight in kilogrammes, L is body length in centimeters, and a and b are constants. Species-specific a and b values from Doidge (1990). For those species whose a and b values Doidge (1990) did not provide we used the values that Schultz (1938) provided to estimate the weights of sharks and whales. We took postnatal *S. scrofa* weight to be the mean weight of the youngest age category ("young pigs before the typical market weight was achieved", ≥ 5 months old) provided by Mutua et al. (2011). We estimated foetal *S. scrofa* weights using the Pomeroy (1960) prediction equation for estimating foetal weight. We could not estimate the weight of the histological *Delphinus* specimen because only a crown-rump length was provided, or of histological *M. novaeangliae* specimens because no length data were provided. We obtained adult body weight data from Spoor et al. (2002).

4.4   Statistical Analysis

We analysed body labyrinth shape deviations between foetal and adult cetacean specimens, adult odontocete and adult mysticete specimens, foetal and adult *S. scrofa* specimens, and adult cetacean and adult *S. scrofa* specimens by comparing the various groups graphically and/or using Mann-Whitney U tests. We performed all statistical analyses using RStudio 0.97.312.

5   Results

5.1   Bony labyrinth ossification

The bony labyrinth produced enough thresholding contrast to enable three-dimensional reconstruction for some foetal cetacean specimens with body lengths >19cm and ossified or cartilaginous bony labyrinths, and both foetal *S. scrofa* specimens (Table 1). None of the bony labyrinths of the histological specimens were ossified; all were cartilaginous. The bony labyrinth was densely ossified in all adult cetacean

²⁴⁸ and *S. scrofa* specimens as well as in the postnatal *S. scrofa* specimen.

²⁴⁹ The largest foetal cetacean specimen in absolute length (27 percent newborn
²⁵⁰ total length, *D. leucas*, ZMB 85708) had a clearly ossified bony labyrinth. Visual
²⁵¹ inspection via μCT images showed that this specimen's bony labyrinth was not
²⁵² as densely ossified as the adult *D. leucas* specimen, however. The largest foetal
²⁵³ cetacean specimen in percentage of newborn total length (42 percent newborn total
²⁵⁴ length, *Delphinus sp.*, ZMB 85736) also had a clearly ossified bony labyrinth. The
²⁵⁵ largest foetal *S. scrofa* specimen (82 percent newborn total length, UMZC2014.7.1)
²⁵⁶ had a clearly ossified bony labyrinth, though visual inspection via μCT images
²⁵⁷ showed that its bony labyrinth was also not as densely ossified as the adult *S.*
²⁵⁸ *scrofa* specimen.

²⁵⁹ All *S. scrofa*, cetacean adults, one cetacean subadult specimen, and six cetacean
²⁶⁰ whole foetuses had sufficiently visible bony labyrinths to enable three-dimensional
²⁶¹ reconstruction of both the semicircular canals and the cochlea. The cetacean
²⁶² specimens were *D. leucas*, *D. delphis*, *Delphinus sp.*, and *P. phocoena* foetuses
²⁶³ of between 15 and 42 percent newborn total length and a subadult (26cm) *M.*
²⁶⁴ *novaeangliae* skull. When specimens' bony labyrinths were cartilaginous, the small
²⁶⁵ difference in threshold values between the soft tissues and air as well as the small
²⁶⁶ diameters of the semicircular canal lumina caused the semicircular canals to be
²⁶⁷ indistinguishable from the bony labyrinth's grainy surface. In these cases we could
²⁶⁸ not identify the semicircular canals with confidence. However, our histological data
²⁶⁹ show that they are pre-formed in cartilage at much smaller developmental stages
²⁷⁰ than those of our μCT-scanned specimens (e.g. *Delphinus sp.* of 14cm CRL).

²⁷¹ 5.2   Bony labyrinth morphology and measurements

²⁷² 5.2.1   Cochlea

²⁷³ Foetal *D. leucas* and *P. phocoena* of as little as 13 and 33 percent newborn total
²⁷⁴ length had the same number of cochlear turns as did adults. Comparing foetal
²⁷⁵ and juvenile *D. delphis* and *M. novaeangliae* specimens to adults of those species
²⁷⁶ in the published literature (*D. delphis*, Solntseva, 2010; *M. novaeangliae*, Ketten,
²⁷⁷ 1994), showed that foetal and adult specimens of both species had almost the same
²⁷⁸ number of cochlear turns as well.

In contrast to the very adult-like cochlear turns among foetuses, cochlear slant heights for foetal cetacean specimens with cochleae that were visible (though not necessarily ossified) in μCT were smaller than those of adult specimens (Figure 2). The largest foetal cetacean specimen in absolute length (27 percent newborn total length, *D. leucas*, ZMB 85708) had a cochlear slant height of 65 percent of the mean adult slant height. The largest foetal cetacean specimen in percentage of newborn total length (42 percent newborn total length, *Delphinus sp.*, ZMB 85736) exhibited a more adult-like slant height of 79 percent of the mean adult slant height. All foetal cetacean specimens had cochlear slant heights of at least 42 percent of the mean adult cochlear slant height.

Cochlear turn diameters in foetal cetacean specimens were smaller than those of adult cochleae. The largest foetal cetacean specimen in absolute length had first and second cochlear turn diameters of 81 and 88 percent the length of the mean adult first and second cochlear turn diameters. The largest foetal cetacean specimen in percentage of newborn total length had first and second cochlear turn diameters of 49 and 42 percent the length of the mean adult first and second cochlear turn diameters. Most foetal cetacean specimens had cochlear turn diameters of at least 33 percent of the mean adult size, with the exception of the histological *Delphinus* sp., *M. novaeangliae*, and *Balaenoptera sp.* specimens.

Overall cochlear size of foetal cetacean specimens was between 38 and 75 percent that of adult specimens. The largest foetal cetacean specimen in absolute length and the largest foetal cetacean specimen in percentage of newborn total length had overall cochlear sizes of 75 and 59 percent adult size respectively.

Both foetal *S. scrofa* specimens (78 and 82 percent of newborn total length) had nearly the same number of cochlear turns (3.25) as did the adult specimen (3.5), while the postnatal *S. scrofa* specimen had the same number of cochlear turns as did the adult specimen. The foetal and postnatal *S. scrofa* specimens had adult-sized cochlear slant heights, and overall cochlea sizes and first, second, and third cochlear turn diameters close to (at least 69 percent of) the mean adult sizes. Meanwhile, the *S. scrofa* histological specimen of 48 percent newborn total length had first and second cochlear turn diameters that were about half the adult size, and a third cochlear turn diameter that was 81 percent the adult size (Table 1).

5.2.2 Semicircular canal radius of curvature

The semicircular canals were visible in eleven of the foetal and embryonic cetacean specimens in this study — six of the whole foetuses, one subadult specimen, and all four of the histological specimens. Only the posterior semicircular canal was visible in one whole foetal specimen (ZMB 85718), while all three canals were visible in the others. Of the whole foetuses, all had mean semicircular canal radii of at least 51 percent that of the mean adult semicircular canal radii. The largest foetal cetacean specimen in absolute length (27 percent newborn total length, *D. leucas*, ZMB 85708) had a mean semicircular canal radius of 66 percent adult size. The largest foetal cetacean specimen in percentage of newborn total length (42 percent newborn total length, *Delphinus sp.*, ZMB 85736) had a mean semicircular canal radius of 65 percent adult size. The subadult *M. novaengliae* skull (26 percent adult skull length) with a near-adult-sized cochlea had an adult-sized mean semicircular canal radius.

Both foetal *S. scrofa* specimens as well as the postnatal specimen had mean semicircular canal radii that were approximately adult-sized.

Table 1 provides each specimen's percent adult size for each bony labyrinth variable, while Figure 3 shows these percentages for cochlear variables of the *D. leucas* foetal specimens, the species for which we had the greatest number of foetuses with visible bony labyrinths in μCT.

5.2.3 Bony labyrinth shape

Neither the ratios of cochlear measurements (slant height, first turn diameter, second turn diameter) to mean semicircular canal radius of curvature, nor the ratios of these cochlear measurements to each other (e.g., first turn diameter : second turn diameter), were significantly different between adult and foetal odontocete specimens (Figure 4, Figure 5, Table 2). In contrast, the ratio of cochlear first to second turn diameter, the only ratio available for foetal mysticetes, was significantly different between adult and foetal mysticete specimens ($p < 0.05$, Table 2). We included all available odontocete or mysticete species in each ratio calculation.

Ratios between cochlear measurements and mean semicircular canal radius of curvature were significantly different between adult odontocete and adult mys-

ticete specimens for all cochlear measurements except for second turn diameter (p
< 0.001 for all, Table 2). Ratios between cochlear slant height and second turn
diameter and between first and second turn diameter were significantly different
between adult odontocete and adult mysticete specimens (p< 0.001 for both ratios,
Figure 5, Table 2). The ratio between cochlear slant height and first turn diam-
eter was not significantly different between adult odontocete and adult mysticete
specimens (Table 2).

Sample sizes were insufficient to identify ratio differences between foetal and
adult *S. scrofa* via a Mann-Whitney U test, but comparing the foetal and post-
natal ratios to adult ratios graphically suggests that ratios are unlikely to be very
different between the two groups (Figure 4, Figure 5).

6   Discussion

This study sought to apply a quantitative lens to how embryonic and foetal inner
ear morphologies change during cetacean gestation as well as that of a closely
related artiodactyl. We asked both when the form and ossification of the bony
labyrinth would emerge during cetacean development, and what the bony labyrinth
growth trajectory would look like. Our results provide four major insights:

First, bony labyrinth ossification onset has occurred in *D. delphis* at around
32 percent of their 280-day intrauterine development period, based on the Stěrba
et al. (2000) staging and aging classification of embryos and foetuses. At this stage,
the foetuses have attained a body length of at least 24cm, or 29 percent of their
approximately 84cm reported newborn total length. Bony labyrinth ossification in
D. leucas had begun as early as at 15 percent of *D. leucas* newborn total length.

Second, cetacean bony labyrinth elements have not achieved full adult size by
the time of ossification onset; size maturation continues thereafter. For example,
ossified specimens such as AMNH 31735 (*M. novaeangliae*, subadult skull) and
ZMB 85708 (*D. leucas*, 27 percent newborn total length) have overall cochlear
sizes of 75 percent of their respective adult sizes.

Third, bony labyrinth shape, as measured by the ratio of cochlear measure-
ments to mean semicircular canal radius of curvature and of cochlear measurements
to each other, does not significantly differ between adult and foetal odontocetes in

our sample. It significantly differs between adult odontocetes and adult mysticetes, and the ratios between first and second cochlear turn diameters significantly differ between adult and foetal mysticetes. Foetal cochleae demonstrate comparable numbers of turns to those of adult cochleae. They are, however, compressed along the central axis — that is, they have a lower slant height — compared to adult cochleae (Figure 2). Foetal cochlear and semicircular canal arc size reach near-adult proportions early in ontogeny (e.g. at 27 percent newborn total length in *D. leucas*).

Fourth, the *S. scrofa* bony labyrinth has ossified and reached near-adult proportions at 82 percent of its gestation period, when the foetus has attained 78 percent of its 29cm newborn total length. The bony labyrinth has not yet ossified or reached adult proportions at 55 percent of the gestation period, which is when the foetus has attained 48 percent of its newborn total length. However, that a foetal cochlea at 55 percent of the gestation period has a nearly equal ratio of first to second cochlear turn diameters to that of an adult *S. scrofa* suggests that the *S. scrofa* bony labyrinth may have attained an adult shape (though not necessarily size) at this stage of development. Data for a cetacean bony labyrinth at an equivalent stage of the gestation period were not available for comparison.

6.1 Bony labyrinth ossification and size maturation

As in previous comparative analyses of developmental sequences (e.g. Nunn & Smith, 1998; Smith, 2001; Hautier et al. 2012), we do not assume linearity in development, or that ontogenetic events (such as ossification or attainment of adult proportions in different parts of the skeleton) should happen at the same relative time in different species. Rather, we have collected data to test whether or not they do. Our results suggest that bony labyrinth ossification has begun by the time cetacean foetuses have undergone 32 percent of their intrauterine development period — that is, by ontogenetic Stage 12 of the Stěrba et al. (2000) staging and aging classification of embryos and foetuses. The finding of Moran et al. (2011) that the otic capsule of *Stenella attenuata* is not yet ossified at Stage 23 of Thewissen & Heyning (2007) (which corresponds to Stage 10 and 11 in the Stěrba et al. (2000) classification — stages that actually *succeed* Stage 12) suggests that ossification is

unlikely to have occurred prior to Stage 12. In contrast, bony labyrinth ossification does not occur in *S. scrofa* until after 55 percent of gestation has occurred, showing that as a proportion of gestation time, bony labyrinth ossification occurs earlier in cetaceans than in *S. scrofa*. Bony labyrinth ossification also begins proportionally earlier in cetaceans than in humans, whose cochlea and semicircular canals only begin to ossify at 40 and 60 percent of the gestation period respectively (Spector & Ge, 1993). Yamato & Pyenson (2015) note that cetacean ears are the most densely ossified skull bones at roughly 20 and 40 percent of newborn total lengths in mysticetes and odontocetes respectively.

Our results also demonstrate that cetacean bony labyrinth size maturation — cochlear slant height, cochlear turn diameter, and semicircular canal radius — continues post-ossification, suggesting a difference between cetacean and human bony labyrinth growth. Jeffery & Spoor (2004) showed that there are few discernible shape changes to the modern human bony labyrinth after otic capsule ossification, though Cox & Jeffery (2007) observed minor reorientation of the semicircular canals during growth, and Spector & Ge (1993) note that the human otic capsule achieves adult size before ossification occurs. Human inner ears are therefore closer to adult form than are cetacean inner ears when ossification occurs.

Starck (1994) suggests that that ossification limits the rate of post-hatching growth in birds — cartilage facilitates faster growth than does bone, whose histogenesis involves several differentiation stages. Applying this principle to cetacean inner ear growth, the cetacean inner ear seems to limit its growth before attaining full adult size by ossifying at sub-adult size and then continuing its growth to full adult size under the constraints of ossification, while the human ear grows as cartilage — presumably at a higher growth rate than that of an ossified cetacean ear — and stops growing when ossified. The ossified foetal *S. scrofa* bony labyrinths we examined were of adult or very near-adult size, suggesting that they may be similar to the modern human bony labyrinth in achieving adult size before ossification occurs. Further study could test this by measuring the bony labyrinth dimensions of newly-ossified *S. scrofa* specimens.

The cetacean bony labyrinth ossification onset time — as early as at 32 percent of the gestation period — agrees with the suggestion by Bruce (1941) and Hautier et al. (2012) that ossification tends to begin earlier as a proportion of

gestation time in species with longer gestation times. As a proportion of gestation time, cetaceans exhibit early ossification onset relative to rodents and terrestrial artiodactyls (e.g. *S. scrofa*). According to Stěrba et al. (2000), the bones of the braincase, face, clavicle, chondrocranium, vertebral arches, ribs, and long limb bones have begun to ossify by Stage 9 (29 percent of the gestation period in *D. delphis*, though note that the long bones have ossified by Stage 9 in all species studied by Stěrba et al. (2000) except *D. delphis*). Moran et al. (2011) similarly found that many of the *S. attenuata* skull bones, but not the otic capsule, had begun to ossify by Stage 9. With our finding that bony labyrinth ossification occurs at Stage 12 or 32 percent of the gestation period, we can infer that bony labyrinth ossification begins after that of many other skeletal elements, and hence that a large portion of ossification has begun by the time of bony labyrinth ossification onset. This suggests that, like *Loxodonta africana* (see Hautier et al. 2012) and other mammals with prolonged gestation times, many cetacean skeletal elements have experienced ossification onset by the end of the first third of gestation — relatively early compared to mammalian groups such as rodents, in which ossification onset continues to occur well into the final third of gestation (Hautier et al., 2012).

Long gestation periods correlate with precocial development in mammals (Zeveloff & Boyce, 1980; Martin & MacLarnon, 1985; Derrickson, 1992). Cetaceans are unusual among other precocial neonates in having to locomote independently "at the instant of birth" (Dearolf et al. 2000). Developmental traits that likely facilitate this ability include the adult or near-adult size and shape of the tympanic bulla and periotic in subadult cetaceans (de Buffrenil et al. 2004; Rauschmann et al. 2006; Lancaster et al. 2015) and precocial and positively allometric locomotor muscle development (Dearolf et al. 2000; McLellan et al. 2002), among others. Our study finds precocial ossification and size maturation of the bony labyrinth even in the prenatal phase of development. This precocial prenatal ossification and growth of the bony labyrinth may offer protection for other inner ear structures that must be well-developed at birth to enable sensory control of locomotion and detection of acoustic cues. Further work on the prenatal ontogeny of non-skeletal inner ear structures such as the basilar membrane would provide further insight into this possibility.

That the *S. scrofa* bony labyrinth has ossified and reached adult proportions at 82 percent, but not 55 percent, of the gestation period suggests that the *S. scrofa* bony labyrinth reaches adult-like ossification levels and size later than the cetacean labyrinth, but earlier than that of rodents. Inner ear ossification centers only appear postnatally in *Mesocricetus auratus*, for example (van Arsdel & Hillemann, 1951). Again, this finding corroborates the ossification onset-gestation time link of Bruce (1941) and Hautier et al. (2012), given that *S. scrofa* periotics are among the last cranial elements to ossify (Nunn & Smith 1998). Though our study demonstrates a difference in the timing (as a percentage of gestation) of a developmental event between cetaceans and a closely related artiodactyl, further work that examines a sequence of additional developmental events alongside bony labyrinth ossification in both taxa would be necessary to investigate further details of sequence heterochrony (Smith, 2001; see also Galatius et al. 2006; Galatius, 2010; Galatius & Gol'din, 2011 for work on cetacean heterochrony).

6.2   Bony labyrinth shape

Though limited size maturation continues post-ossification, bony labyrinth shape does not significantly differ between adult and foetal odontocetes. Foetal odontocetes already exhibit adult-like cochlear coiling. Indeed, Solntseva (1999, 2002) notes that the complete anatomical formation of mammalian cochleae typically occurs before the ear capsule turns cartilaginous. The cetacean cochlea and semicircular canals also reach near-adult size early in ontogeny (e.g. at 27 percent newborn total length in *D. leucas*). This suggests that the odontocete bony labyrinth achieves adult shape characteristics relatively early in the gestation period. Further, it shows that a particularly derived cetacean trait — that of relatively small semicircular canals — appears early in ontogeny. The only discernible shape change between adult and foetal odontocetes was that of cochlear slant height, which was significantly different between adult and foetal odontocete species (p < 0.001). Visual inspection of three-dimensional bony labyrinth reconstructions shows the foetal cochleae as flattened compared to the more sharply-pointed organs of adults (Figure 2). Potential functional explanations for this remain unknown. The lengthening of the cochlear spiral along the central axis during development

may reflect some frequency range expansion, but without a method for establishing cetacean frequency ranges according to cochlear dimensions this possibility remains unexplored.

The ratio of first to second cochlear turn diameter was significantly different between adult and foetal mysticetes ($p < 0.05$, note that mysticete adult and foetal ratios were calculated using μCT and histology respectively due to a lack of visible mysticete foetal bony labyrinths in μCT data). The less adult-like shape of the foetal mysticete cochlea compared to the foetal odontocete cochlea may reflect the accelerating development that occurs in mysticetes at and after the transition from embryo to foetus (Roston et al. 2013). The histological mysticete specimens we examined all had cartilaginous bony labyrinths, and the *Balaenoptera sp.* specimen (the only histological mysticete specimen for which a length measurement was available) had a TL of only 13.7cm, consistent with these specimens' early, embryonic stage of development.

Meanwhile, a foetal *S. scrofa* cochlea at 55 percent of the gestation period has nearly equal first to second cochlear turn, first to third cochlear turn, and second to third cochlear turn diameter ratios as an adult *S. scrofa* cochlea, suggesting that the *S. scrofa* bony labyrinth may have attained an adult shape at this stage of development.

Bony labyrinth shape was significantly different between adult odontocetes and adult mysticetes for all ratios ($p < 0.001$) except those between cochlear second turn diameter and mean semicircular canal radius of curvature, and between cochlear slant height and first turn diameter. This result likely relates to the different modes of coiling of odontocete and mysticete cochleae. Ketten (1992) describes two odontocete modes: Type I cochleae have spirals that resemble "tightly coiled rope", while Type II cochleae have logarithmic spirals that are more elongated along the central axis. Mysticete cochleae are more elongated along the central axis than those of both odontocete types, and are not coiled in one plane (Fleischer, 1976; Ketten, 1992). Fleischer (1976) suggests that a low height to diameter ratio of the cochlea (which describes odontocete cochleae more than mysticete ones) helps cetaceans to detect high frequencies. Further, Fleischer (1976) notes that the basal end of some odontocete cochleae curve in a different direction from the rest of the cochlear coiling, a countercurvature that mysticete cochleae can also possess to

534 a smaller extent. Our results suggest that there is a significant difference between
535 the cochlear slant height to second turn diameter ratios of odontocetes and mys-
536 ticetes (the ratio is lower for odontocetes than for mysticetes), but not between the
537 cochlear slant height to first turn diameter ratios of odontocetes and mysticetes.
538 This disparity may arise because of the different definitions of "diameter" between
539 this paper and that of Fleischer (1976), or because of the countercurvature of
540 odontocete cochleae that Fleischer (1976) observed. Text-fig. 1 in Fleischer (1976)
541 and fig. 35.10 in Ketten (1992) provide useful illustrations of the different shapes
542 and modes of coiling between odontocete and mysticete cochleae.

6.3 Inner ear growth allometry and Conclusions

Negative allometry is a common scaling pattern for cetacean skull elements (see Read & Tolley, 1997; McLellan et al. 2002; Spoor et al. 2002). Our results demonstrate that foetal cochlear and semicircular canal size scale with body mass with strong negative allometry, as generally observed for sensory organs throughout vertebrates. *D. leucas* specimens as small as 15 percent of newborn length have cochleae of 68 and 60 percent adult cochlear and semicircular canal size respectively (Table 1). The observed negative allometry of bony labyrinth growth in cetaceans may simply reflect "some form of spatial constraint of otic capsule growth" within the skull (Spoor 2014, pers. comm.).

Cetaceans face a unique challenge among mammals in needing to perform a great many life processes entirely in water and being unable to survive outside of the medium. It is thus important to adequately understand the morphological features of the hearing and vestibular apparatus, key systems that make survival possible, in order to better understand the factors that have contributed to their remarkable success in achieving independence from land. We have sought to shed light on the developmental processes of some of these peculiarities, and discuss how they fit into the broader picture of cetacean life history. Inner ear ontogeny is a useful character with which to examine mammalian development, and our results on cetaceans further underscores this order's uniqueness among mammals.

7 Acknowledgements

580   8   Author Contributions

581 T.T. and R.J.A. conceived the study. N.K., T.T., and R.J.A. performed μCT scan-
582 ning. T.T. collected histological data, collected measurements from the μCT and
583 histological data, analyzed and interpreted the data, and wrote the manuscript.
584 R.J.A. supervised the project, assisted with data interpretation, and helped to
585 write the manuscript.

References

Armfield BA, George JC, Vinyard CJ, Thewissen JGM (2011) Allometric patterns
of fetal head growth in mysticetes and odontocetes: Comparison of *Balaena
mysticetus* and *Stenella attenuata*. *Mar Mamm Sci* **27**, 819–827.

Bruce JA (1941) Time and order of appearance of ossification centers and their
development in the skull of the rabbit. *Am J Anat* **68**, 41–67.

Clark ST, Odell DK (1999) Allometric Relationships and Sexual Dimorphism in
Captive Killer Whales (*Orcinus orca*). *J Mammal* **80**, 777–785.

Cock AG (1966) Genetical Aspects of Metrical Growth and Form in Animals. *Q
Rev Biol* **41**, 131–190.

Cox PG, Jeffery N (2007) Morphology of the Mammalian Vestibulo-Ocular Re-
flex: The Spatial Arrangement of the Human Fetal Semicircular Canals and
Extraocular Muscles. *J Morphol* **268**, 878–890.

de Buffrenil V, Dabin W, Zylberberg L (2004) Histology and growth of the cetacean
petro-tympanic bone complex. *J Zool* **262**, 371–381.

Dearolf JL, McLellan WA, Dillaman RM, Frierson D, Pabst DA (2000) Precocial development of axial locomotor muscle in bottlenose dolphins (*Tursiops truncatus*). *J Morphol* **244**, 203–215.

Derrickson EM (1992) Comparative Reproductive Strategies of Altricial and Precocial Eutherian Mammals. *Funct Ecol* **6**, 57–65.

Doidge DW (1990) Age and stage based analysis of the population dynamics of beluga whales, *Delphinapterus leucas*, with particular reference to the northern Quebec population. Ph.D. thesis, McGill University.

Dunkin RC, McLellan WA, Blum JE, Pabst DA (2005) The ontogenetic changes in the thermal properties of blubber from Atlantic bottlenose dolphin *Tursiops truncatus*. *J Exp Biol* **208**, 1469–1480.

Fleischer G (1976) Hearing in extinct cetaceans as determined by cochlear structure. *J Paleontol* **50**, 133–152.

Galatius A (2010) Paedomorphosis in two small species of toothed whales (Odontoceti): how and why? *Biol J Linnean Soc* **99**, 278–295.

Galatius A, Andersen MER, Haugan B, Langhoff HE, Jespersen Å (2006) Timing of epiphyseal development in the flipper skeleton of the harbour porpoise (*Phocoena phocoena*) as an indicator of paedomorphosis. *Acta Zool* **87**, 77–82.

Galatius A, Gol'din PE (2011) Geographic variation of skeletal ontogeny and skull shape in the harbour porpoise (*Phocoena phocoena*). *Can J Zool* **89**, 869–879.

Gatesy J, Milinkovitch M, Waddell V, Stanhope M (1999) Stability of Cladistic Relationships between Cetacea and Higher-Level Artiodactyl Taxa. *Syst Biol* **48**, 6–20.

Geisler JH, Luo Z (1996) The petrosal and inner ear of *Herpetocetus* sp.(Mammalia: Cetacea) and their implications for the phylogeny and hearing of archaic mysticetes. *J Paleontol* **70**, 1045–1066.

Gingerich PD, ul Haq M, Zalmout IS, Khan IH, Malkani MS (2001) Origin of whales from early artiodactyls: hands and feet of Eocene Protocetidae from Pakistan. *Science* **293**, 2239–2242.

Gray AA (1907) *The Labyrinth of Animals*, vol. 1. London: J. & A. Churchill.

Hautier L, Stansfield FJ, Allen WT, Asher RJ (2012) Skeletal development in the African elephant and ossification timing in placental mammals. *Proc R Soc Lond B Biol Sci* **279**, 2188–2195.

Jefferson TA, Leatherwood S, Webber MA (1993) *Marine mammals of the world.* Rome: Food & Agriculture Organization of the United Nations.

Jeffery N, Spoor F (2004) Prenatal growth and development of the modern human labyrinth. *J Anat* **204**, 71–92.

Kandel M, Hullar TE (2010) The relationship of head movements to semicircular canal size in cetaceans. *J Exp Biol* **213**, 1175–1181.

Ketten DR (1992) The Marine Mammal Ear: Specializations for Aquatic Audition and Echolocation. In: *The Evolutionary Biology of Hearing.* (eds. Webster DB, Fay RR, Popper AN), pp. 717–750, New York: Springer-Verlag.

Ketten DR (1994) Functional analyses of whale ears: adaptations for underwater hearing. *IEEE Proc Underwater Acoust* **1**, 264–270.

Ketten DR, Wartzok D (1990) Three-dimensional reconstructions of the dolphin ear. In: *Sensory Abilities of Cetaceans.* (eds. Thomas JA, Kastelein RA), pp. 81–105, New York: Plenum Press.

Kinkel MD, Thewissen JGM, Oelschläger HA (2001) Rotation of middle ear ossicles during cetacean development. *J Morphol* **249**, 126–131.

Klima M (1995) Cetacean phylogeny and systematics based on the morphogenesis of the nasal skull. *Aquat Mammal* **21**, 79–89.

Lancaster WC, Ary WJ, Krysl P, Cranford TW (2015) Precocial development within the tympanoperiotic complex in cetaceans. *Mar Mamm Sci* **31**, 369–375.

Lindenlaub T, Oelschläger HA (2000) Preliminary observations on the morphology of the inner ear of the fetal narwhal (*Monodon monoceros*). *Hist Biol* **14**, 47–51.

Lovell JM, Harper GM (2007) The morphology of the inner ear from the domestic pig (*Sus scrofa*). *J Microsc* **228**, 345–357.

Lu X (2003) Postnatal growth of skull linear measurements of Cape hare Lepus capensis in northern China: an analysis in an adaptive context. *Biol J Linnean Soc* **78**, 343–353.

Martin RD, MacLarnon AM (1985) Gestation period, neonatal size and maternal investment in placental mammals. *Nature* **313**, 220–223.

McLellan WA, Koopman HN, Rommel SA, Read AJ, Potter CW, Nicolas JR, et al. (2002) Ontogenetic allometry and body composition of harbour porpoises (*Phocoena phocoena*, L.) from the western North Atlantic. *J Zool* **257**, 457–471.

Melin AD, Bergmann PJ, Russell AP (2005) Mammalian Postnatal Growth Estimates: The Influence of Weaning on the Choice of a Comparative Metric. *J Mammal* **86**, 1042–1049.

Moran MM, Nummela S, Thewissen JGM (2011) Development of the skull of the pantropical spotted dolphin (*Stenella attenuata*). *Anat Rec* **294**, 1743–1756.

Mutua FK, Dewey CE, Arimi SM, Schelling E, Ogara WO (2011) Prediction of live body weight using length and girth measurements for pigs in rural Western Kenya. *J Swine Health Prod* **19**, 26–33.

Nunn CL, Smith KK (1998) Statistical analyses of developmental sequences: the craniofacial region in marsupial and placental mammals. *Amer Nat* **152**, 82–101.

Ohsumi S (1966) Allomorphosis between body length at sexual maturity and body length at birth in the Cetacea. *J Mamm Soc Japan* **3**, 3–7.

Pomeroy RW (1960) Infertility and neonatal mortality in the sow III. Neonatal mortality and foetal development. *J Agric Sci* **54**, 31–56.

Rauschmann MA, Huggenberger S, Kossatz LS, Oelschlger HH (2006) Head morphology in perinatal dolphins: A window into phylogeny and ontogeny. *J Morphol* **267**, 1295–1315.

Read AJ, Tolley KA (1997) Postnatal growth and allometry of harbour porpoises from the Bay of Fundy. *Can J Zool* **75**, 122–130.

Rose KD (2006) *The Beginning of the Age of Mammals.* Maryland: Johns Hopkins University Press.

Roston RA, Lickorish D, Buchholtz EA (2013) Anatomy and age estimation of an early blue whale (*Balaenoptera musculus*) fetus. *Anat Rec* **296**, 709–722.

Schultz LP (1938) Can the Weight of Whales and Large Fish be Calculated? *J Mammal* **19**, 480–487.

Silcox MT, Bloch JI, Boyer DM, Godinot M, Ryan TM, Spoor F, et al. (2009) Semicircular canal system in early primates. *J Hum Evol* **56**, 315–327.

Smith KK (2001) Heterochrony revisited: the evolution of developmental sequences. *Biol J Linn Soc* **73**, 169–186.

Solntseva GN (1990) Formation of an Adaptive Structure of the Peripheral Part of the Auditory Analyzer in Aquatic, Echo-Locating Mammals During Ontogenesis. In: *Sensory Abilities of Cetaceans* (eds. Thomas JA, Kastelein RA), pp. 363–383, New York: Plenum Press.

Solntseva GN (1999) Development of the auditory organ in terrestrial, semi-aquatic, and aquatic mammals. *Aquatic Mammals* **25**, 135–148.

Solntseva GN (2002) Early embryogenesis of the vestibular apparatus in mammals with different ecologies. *Aquatic Mammals* **28**, 159–169.

Solntseva GN (2010) Morphology of the inner ear of mammals in ontogeny. *Russ J Dev Biol* **41**, 94–110.

Spaulding M, O'Leary MA, Gatesy J (2009) Relationships of Cetacea (Artiodactyla) among mammals: increased taxon sampling alters interpretations of key fossils and character evolution. *PLoS One* **4**, e7062.

Spector JG, Ge X (1993) Ossification patterns of the tympanic facial canal in the human fetus and neonate. *Laryngoscope* **103**, 1052–1065.

Spoor F, Bajpai S, Hussain ST, Kumar K, Thewissen JG (2002) Vestibular evidence for the evolution of aquatic behaviour in early cetaceans. *Nature* **417**, 163–166.

Spoor F, Thewissen JGM (2008) Comparative and Functional Anatomy of Balance in Aquatic Mammals. In: *Sensory Evolution on the Threshold: Adaptations in Secondarily Aquatic Vertebrates*, pp. 257–284, Berkeley: University of California Press Berkeley, California.

Spoor F, Zonneveld F (1995) Morphometry of the primate bony labyrinth: a new method based on high-resolution computed tomography. *J Anat* **186**, 271–286.

Starck JM (1994) Quantitative design of the skeleton in bird hatchlings: Does tissue compartmentalization limit posthatching growth rates? *J Morphol* **222**, 113–131.

Struthers J (1889) *Memoir on the Anatomy of the Humpback Whale,* Megaptera Logimana. Edinburgh: Maclachlan and Stewart.

Stěrba O, Klima M, Schildger B (2000) Embryology of Dolphins. Staging and Ageing of Embryos and Fetuses of Some Cetaceans. *Adv Anat Embryol Cell Biol* **157**, 1–133.

Thewissen JGM, Heyning J (2007) Embryogenesis and development in *Stenella attenuata* and other cetaceans. In: *Reproductive Biology and Phylogeny of Cetacea: Whales, Dolphins, and Porpoises*, pp. 307–329, New Hampshire: Science Publishers.

Thewissen JGM, Williams EM, Roe LJ, Hussain ST (2001) Skeletons of terrestrial cetaceans and the relationship of whales to artiodactyls. *Nature* **413**, 277–281.

Tsai C, Fordyce RE (2014) Disparate Heterochronic Processes in Baleen Whale Evolution. *Evol Biol* **41**, 299–307.

Ullrey DE, Sprague JI, Becker DE, Miller ER (1965) Growth of the swine fetus. *J Anim Sci* **24**, 711–717.

van Arsdel WC, Hillemann HH (1951) The ossification of the middle and internal ear of the golden hamster (*Cricetus auratus*). *Anat Rec* **109**, 673–689.

Yamato M, Pyenson ND (2015) Early Development and Orientation of the Acoustic Funnel Provides Insight into the Evolution of Sound Reception Pathways in Cetaceans. *PloS One* **10**, e0118582.

Zeveloff SI, Boyce MS (1980) Parental investment and mating systems in mammals. *Evolution* **34**, 973–982.

Table 1: Size, cochlear and semicircular canal dimensions relative to those of adult inner ears, and number of cochlear turns for all specimens.

SPECIES	COMMON NAME	SPECIMEN	SIZE (m)	% NEW-BORN TL	OSSIFIED	% ADULT SIZE C	SH	D1	D2	D3	R	TURNS
Delphinapterus leucas	Beluga whale	ZMB 85701	0.25	17	N	63	58	64	67	NA	NA	2
Delphinapterus leucas	Beluga whale	ZMB 85702	0.20	13	N	65	55	80	50	NA	NA	2
Delphinapterus leucas	Beluga whale	ZMB 85703	0.25	17	N	53	51	54	53	NA	NA	2
Delphinapterus leucas	Beluga whale	ZMB 85704	0.30	20	N	38	44	33	36	NA	NA	2
Delphinapterus leucas	Beluga whale	ZMB 85708	0.40	27	Y	75	65	81	88	NA	66	2
Delphinapterus leucas	Beluga whale	ZMB 85709	0.23	15	Y	56	42	64	68	NA	60	2
Delphinapterus leucas	Beluga whale	ZMB 85710	0.23	15	Y	68	56	75	79	NA	NA	2
Delphinapterus leucas	Beluga whale	ZMB 85711	0.30	20	N	NA	NA	NA	NA	NA	NA	NA
Delphinapterus leucas	Beluga whale	ZMB 85712	0.20	13	N	NA	NA	NA	NA	NA	NA	NA
Delphinapterus leucas	Beluga whale	ZMB 85714	0.35	23	N	NA	NA	NA	NA	NA	NA	NA

Table 1: Size, cochlear and semicircular canal dimensions relative to those of adult inner ears, and number of cochlear turns for all specimens.

SPECIES	COMMON NAME	SPECIMEN	SIZE (m)	% NEW-BORN TL	OSSIFIED	% ADULT SIZE						TURNS
						C	SH	D1	D2	D3	R	
Delphinus delphis	Short-beaked common dolphin	ZMB 85720	0.25	30	Y	41	50	36	34	NA	53	2
Delphinus delphis	Short-beaked common dolphin	ZMB 4056	0.26	31	N	NA	NA	NA	NA	NA	NA	NA
Delphinus delphis	Short-beaked common dolphin	ZMB 85721	0.10	12	N	NA	NA	NA	NA	NA	NA	NA
Delphinus delphis	Short-beaked common dolphin	ZMB 85722	0.06	7	N	NA	NA	NA	NA	NA	NA	NA
Delphinus sp.	Common dolphin	ZMB 85736	0.35	42	Y	59	79	49	42	NA	65	2
Delphinus sp.	Common dolphin	UT Delphinus1	0.14*	NA	N	NA	NA	43	30	NA	NA	NA
Phocoena phocoena	Harbour porpoise	ZMB 85717	0.25	33	Y	69	71	71	60	NA	77	1.75
Phocoena phocoena	Harbour porpoise	ZMB 85718	0.19	25	Y	62	59	67	58	NA	51	1.5-2
Hyperoodon ampullatus	Northern bottlenose whale	ZMB 85518	0.19	5	N	NA	NA	NA	NA	NA	NA	NA
Megaptera novaeangliae	Humpback whale	ZMB 37784	0.25	6	N	NA	NA	NA	NA	NA	NA	NA

Table 1: Size, cochlear and semicircular canal dimensions relative to those of adult inner ears, and number of cochlear turns for all specimens.

SPECIES	COMMON NAME	SPECIMEN	SIZE (m)	% NEW-BORN TL	OSSIFIED	% ADULT SIZE						TURNS
						C	SH	D1	D2	D3	R	
Megaptera novaeangliae	Humpback whale	ZMB 85515	0.25	6	N	NA	NA	NA	NA	NA	NA	NA
Megaptera novaeangliae	Humpback whale	ZMB 37786	0.35	8	N	NA	NA	NA	NA	NA	NA	NA
Megaptera novaeangliae	Humpback whale	ZMB 85699	0.04	0.9	N	NA	NA	NA	NA	NA	NA	NA
Megaptera novaeangliae	Humpback whale	ZMB 37783	0.10	2	N	NA	NA	NA	NA	NA	NA	NA
Megaptera novaeangliae	Humpback whale	ZMB 85697	0.06	1	N	NA	NA	NA	NA	NA	NA	NA
Megaptera novaeangliae	Humpback whale	AMNH 31735 (skull)	0.26	26 (% new-born skull length)	Y	75	Ad	67	36	NA	Ad	2
Megaptera novaeangliae	Humpback whale	Megaptera serie 1-21	?	NA	N	NA	NA	34	28	NA	NA	NA
Megaptera novaeangliae	Humpback whale	Megaptera IX	?	NA	N	NA	NA	18	14	NA	NA	NA
Balaenoptera borealis	Sei whale	UMZC C.17.M	0.31	7	N	NA	NA	NA	NA	NA	NA	NA
Balaenoptera musculus	Blue whale	UMZC C.14.D	0.28	4	N	NA	NA	NA	NA	NA	NA	NA

Table 1: Size, cochlear and semicircular canal dimensions relative to those of adult inner ears, and number of cochlear turns for all specimens.

SPECIES	COMMON NAME	SPECIMEN	SIZE (m)	% NEW-BORN TL	OSSIFIED	% ADULT SIZE						TURNS
						C	SH	D1	D2	D3	R	
Balaenoptera sp.	Rorqual	UMZC Bp1	0.14	2	N	NA	NA	14	9	NA	NA	NA
Sus scrofa	Wild boar	DPDN 1 (skull)	?	NA	Y	87	Ad	69	90	Ad	99	3.5
Sus scrofa	Wild boar	UMZC 2014.7.1	0.24*	82	Y	86	Ad	77	91	86	99	3.25
Sus scrofa	Wild boar	UMZC 2014.7.2	0.23*	78	Y	86	Ad	78	90	79	96	3.25
Sus scrofa	Wild boar	UT Sus1	0.14*	48	N	NA	NA	52	57	81	NA	NA
Delphinapterus leucas	Beluga whale	Delphinapterus C77F (Adult petrosal)	?	NA	Y	Ad	Ad	Ad	Ad	NA	Ad	2
Phocoena phocoena	Harbour porpoise	Phocoena C80G (Adult petrosal)	?	NA	Y	Ad	Ad	Ad	Ad	NA	Ad	1.75
Sus scrofa	Wild boar	DPDN 2 (Adult skull)	?	NA	Y	Ad	Ad	Ad	Ad	Ad	Ad	3.5

TL, total length; C, overall cochlear size; SH, slant height; D1, first turn diameter; D2, second turn diameter; D3, third turn diameter; R, mean semicircular canal radius of curvature; NA = no measurement due to insufficient bony labyrinth ossification or measurement not taken (e.g. D3 in cetaceans with only two cochlear turns); Ad = Adult; Y = Yes; N = No. "Size" column refers to total length (TL) except where specimen is a skull, adult petrosal,

or size value comes with an asterisks, which denotes crown-rump length. Only a crown-rump length was available for some histological specimens. % newborn TL for *Balaenoptera sp.* taken as percentage of average newborn TL of *B. musculus* and *B. borealis*, since these were the two *Balaenoptera* species included in our dataset. % newborn TL of *D. delphis* calculated as percentage of newborn *Delphinus sp.* TL.

Table 2: P-values of Mann-Whitney U tests of ratios between cochlear parameters and mean semicircular canal radius of curvature, and cochlear parameters and each other.

Data Group	P-values						
	SH : R	D1 : R	D2 : R	C : R	SH : D1	SH : D2	D1 : D2
Adult odontocetes vs foetal odontocetes	0.71	0.98	0.93	1.00	0.72	0.50	0.08
Adult mysticetes vs foetal mysticetes	NA	NA	NA	NA	NA	NA	0.0020
Adult odontocetes vs adult mysticetes	2.7e-05	5.02e-05	0.89	0.00063	0.72	2.4e-05	5.5e-08

Abbreviations as for Table 1.

9   Figure Legends

Figure 1: (a) Measurement of cochlear slant height in an adult *D. leucas* specimen, taken as the distance between the cochlear apex and the topmost edge (furthest from the apex) of the round window (Gray, 1907; Spoor et al. 2002). (b) First and second turn diameter measurements in an adult *D. leucas* specimen in the plane of the ASC arc. Blue line: first turn; red line: second turn. (c) Best fit plane through the ASC arc in an adult *D. leucas* specimen, represented by black line. We translated this best fit plane to the part of the cochlea with the largest diameter of the first and second turns to measure the first and second cochlear turn diameter. Modeled from instructive diagrams by Fred Spoor. (d) Measurement of semicircular canal height and width, as defined by Spoor & Zonneveld (1995). The average of these measurements is then divided by two to obtain the semicircular canal radius of curvature.

Figure 2: Three-dimensional reconstructions of *D. leucas* bony labyrinths over ontogeny: (a) 23cm foetus (b) 40cm foetus (c) Adult. The reconstructions demonstrate the elongation of the *D. leucas* cochlea along its central axis — that is, the increase in cochlear slant height, or apex-round window distance — over ontogeny. Bony labyrinth coiling remains consistent. We removed stray pixels in Figure 6 (a) and (b), and flipped both images so that they faced the same direction as Figure 6 (c) for ease of comparison.

Figure 3: Measurements of cochlear slant height, first and second turn diameters, overall cochlear size, and semicircular canal radius of curvature in six foetal *D. leucas* expressed as percentages of mean adult size. Percentages of newborn total length based on calf data given in Ohsumi (1966) are as follows: ZMB 85709 (15%, blue), ZMB 85710 (15%, pink), ZMB 85701 (17%, orange), ZMB 85703, (17%, ochre), ZMB 85704 (20%, green), ZMB 85708 (27%, turquoise).

Figure 4: Bivariate plots of ratios of cochlear parameters to mean semicircular canal radius of curvature onto logarithmically transformed body mass for adult odontocetes, adult mysticetes, foetal odontocetes, adult *S. scrofa*, and foetal *S. scrofa*. Data points: red, adult odontocetes; blue, adult mysticetes; green, foetal odontocetes; orange, adult *S. scrofa*; purple, foetal *S. scrofa*. Abbreviations: R, mean semicircular canal radius of curvature.

Figure 5: Bivariate plots of ratios of cochlear parameters to each other onto logarithmically transformed body mass for adult odontocetes, adult mysticetes, foetal odontocetes, foetal mysticetes, adult *S. scrofa*, and foetal *S. scrofa*. Data points: red, adult odontocetes; blue, adult mysticetes; green, foetal odontocetes; black, foetal mysticetes; orange, adult *S. scrofa*; purple, foetal *S. scrofa*.
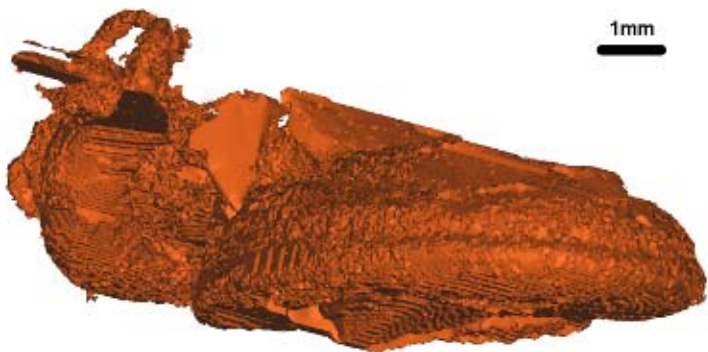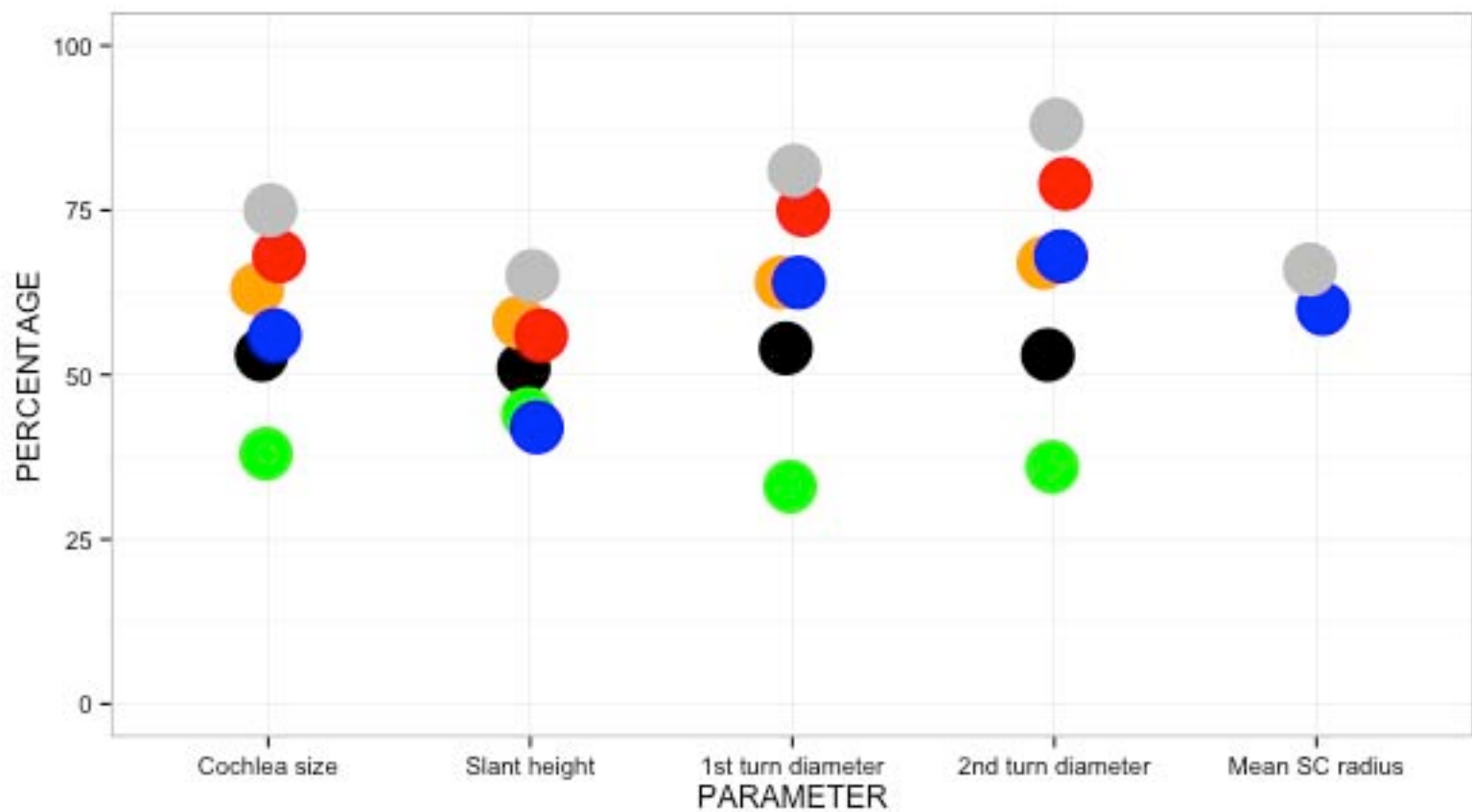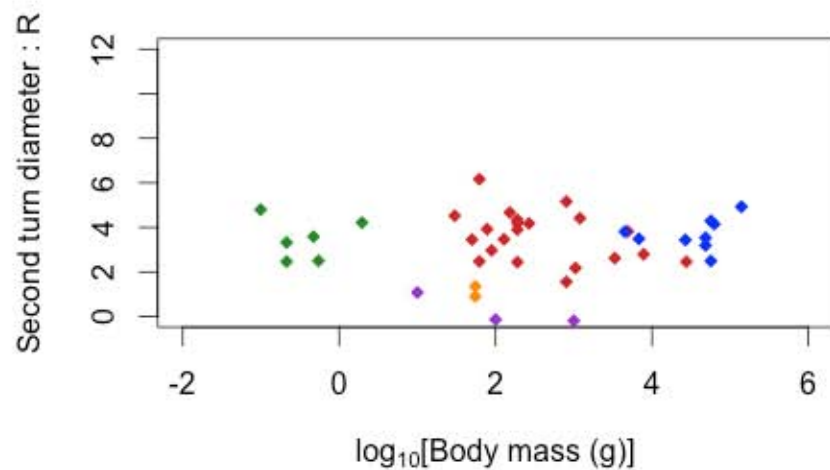
a

round window

apex

b

first turn diameter

second turn diameter

c

psc

lsc

cochlea

d

height

width